AD NUMBER
AD405150
LIMITATION CHANGES
TO: **Approved for public release; distribution is unlimited.**
FROM: **Distribution authorized to U.S. Gov't. agencies and their contractors; Administrative/Operational Use; MAY 1963. Other requests shall be referred to Arnold Engineering Development Center, Arnold AFB, TN 37389.**
AUTHORITY
AEDC ltr, 28 Jul 1965

+A 03 a1

AEDC-TDR-63-87

DUPLICATE

INVESTIGATION OF DRAG REDUCTION BY BOUNDARY-LAYER SUCTION ON A 72.5-DEG SWEPT WING AT $M_\infty = 2$ AND 2.25

By

S. R. Pate and J. S. Deitering

von Kármán Gas Dynamics Facility

ARO, Inc.

TECHNICAL DOCUMENTARY REPORT NO. AEDC-TDR-63-87

May 1963

AFSC Program Area 750A , Project 1366 , Task 136612

(Prepared under Contract No. AF 40(600)-1000 by ARO, Inc., contract operator of AEDC, Arnold Air Force Station, Tenn.)

ARNOLD ENGINEERING DEVELOPMENT CENTER

AIR FORCE SYSTEMS COMMAND

UNITED STATES AIR FORCE

NOTICES

INVESTIGATION OF DRAG REDUCTION BY BOUNDARY-LAYER SUCTION ON A 72.5-DEG SWEPT WING AT M_∞ = 2 AND 2.25

By

S. R. Pate and J. S. Deitering

von Kármán Gas Dynamics Facility

ARO, Inc.

a subsidiary of Sverdrup and Parcel, Inc.

May 1963

ARO Project No. VA0232

ABSTRACT

Tests were conducted in the 40-Inch Supersonic Tunnel (A) of the von Kármán Gas Dynamics Facility to determine the effectiveness of boundary-layer suction for laminar flow control on a two-dimensional, 72.5-deg swept wing having a subsonic leading edge. Test Mach numbers were 2 and 2.25 with a Reynolds number range based on wing chord from 3 to 14 million for angles of attack of 0.15, 0.45, and 0.75 deg.

With suction, full chord laminar flow was maintained at $M_\infty = 2$, $\alpha = 0.15$, 0.45, and 0.75 deg up to a length Reynolds number of approximately 9 million. At $M_\infty = 2.25$ and $\alpha = 0.15$ deg, full chord laminar flow was maintained up to a Reynolds number of 6.5×10^6 and for $\alpha = 0.45$ and 0.75 deg, up to a Reynolds number of 3×10^6. Selected data are presented.

PUBLICATION REVIEW

This report has been reviewed and publication is approved.

Darreld K Calkins

Darreld K. Calkins
Major, USAF
AF Representative, VKF
DCS/Test

Jean A Jack

Jean A. Jack
Colonel, USAF
DCS/Test

CONTENTS

ILLUSTRATIONS

NOMENCLATURE

A_n	Reference area based on n^{th} chamber average span and rake location $(A_n = b_n \cdot x)$, sq in.
b_n	Reference width (average span in n^{th} chamber), in.
C_{D_S}	Suction drag coefficient, $\sum_{n=1}^{x} C_{m_n} \left(1 + \frac{M_n^2 T_n}{M_\infty^2 T_\infty}\right)$
C_{D_T}	Total drag coefficient $(C_{D_W} + C_{D_S})$
C_{D_W}	Wake drag coefficient $(2\theta_\infty/x)$
C_{m_n}	Local suction coefficient, $(m_n/\rho_\infty U_\infty A_n)$
C_{m_t}	Total suction coefficient, $\sum_{n=1}^{x} C_{m_n}$
c	Model chord length, measured parallel to free stream, 33.3 in.
M_n	Suction chamber Mach number
M_r	Mach number outside boundary layer
M_{r_N}	Local Mach number outside boundary layer normal to wing leading edge
M_∞	Free-stream Mach number
m_n	Local mass rate of suction, lb-sec/in.
p	Model surface pressure, psia
p_o	Tunnel stagnation pressure, psia
q_∞	Free-stream dynamic pressure, psia
Re_x	Reynolds number based on rake location (x = 33.3 in.)
T_n	Suction chamber temperature, °R
T_∞	Free-stream static temperature, °R
U_r	Velocity outside boundary layer, ft/sec
U_∞	Free-stream velocity, ft/sec or in./sec
u	Local velocity in boundary layer, ft/sec
x	Model surface coordinate or boundary-layer rake location, measured from model leading edge, in.

y	Model surface coordinate or distance normal to model surface, in.
α	Wing angle of attack, deg
δ	Boundary-layer total thickness, in.
θ_r	Boundary-layer momentum thickness at rake location, in. $\int_0^{\delta} \frac{\rho\, u}{\rho_r\, U_r}\left(1 - \frac{u}{U_r}\right) dy$
θ_∞	Boundary-layer momentum thickness for free-stream conditions, in.
ρ	Local density in the boundary-layer, $\frac{\text{lb-sec}^2}{\text{in.}^4}$
ρ_r	Density outside boundary layer, $\frac{\text{lb-sec}^2}{\text{in.}^4}$
ρ_∞	Free-stream density, $\frac{\text{lb-sec}^2}{\text{in.}^4}$

SUBSCRIPTS

n	The n^{th} suction chamber
r	Conditions outside the boundary layer
∞	Free-stream conditions

1.0 INTRODUCTION

Under the sponsorship of the Aeronautical Systems Division (ASD), Air Force Systems Command (AFSC), a boundary-layer laminar flow control test was conducted on a 72.5-deg, two-dimensional swept wing for the NORAIR Division of the Northrop Corporation. Tests were made in the 40-Inch Supersonic Tunnel (A) of the von Kármán Gas Dynamics Facility (VKF), Arnold Engineering Development Center (AEDC), AFSC, during the period of January 21 to 26, 1963. Test Mach numbers were 2 and 2.25 over a Reynolds number range based on wing chord from 3 to 14 million at angles of attack of 0.15, 0.45, and 0.75 deg.

The purpose of the test was to determine if full-chord laminar flow could be achieved at supersonic speeds with boundary-layer suction on a highly swept wing with a subsonic leading edge and to measure the suction requirements and wake drag.

2.0 APPARATUS

2.1 WIND TUNNEL

The 40-Inch Supersonic Tunnel (A) in Fig. 1 is a continuous, closed circuit, variable density wind tunnel with an automatically driven, flexible-plate-type nozzle. The tunnel operates at Mach numbers from 1.5 to 6 at maximum stagnation pressures from 29 to 200 psia, respectively, and stagnation temperatures up to 300°F ($M_\infty = 6$). Minimum operating pressures are about one-tenth of the maximum at each Mach number. A complete description of the tunnel and airflow calibration information is given in Ref. 1.

2.2 MODEL

The 72.5-deg, NORAIR swept wing (Figs. 2 and 3) was mounted vertically to a horizontal support plate that spanned the tunnel test section and was supported by the tunnel sidewalls. The wing had a subsonic leading edge ($M_\infty \cos 72.5° < 1$) and the characteristics of a high lift subsonic wing. Accordingly, the wing had a subsonic airfoil, which is illustrated in Fig. 4.

Manuscript received April 1963.

The support plate was contoured to the flow field streamlines so that root effects would be negligible and the wing would have two-dimensional characteristics. A section of the top surface was vented with 75 suction slots (parallel to the leading edge and 0.003- and 0.004-in. in width) through which a portion of the boundary layer was removed. Changes in wing angle-of-attack were made by rotating the support plate about a pivot point (see Fig. 3).

Seven separate suction chambers were contained within the model and connected separately to individual metering boxes; thus variable suction was provided over the model surface. The model was instrumented to measure the surface pressure along three spanwise stations with each station having thirteen orifices (see Fig. 4). Ambient pressures were also measured in each of the seven suction chambers, and the temperature was measured in three of the seven chambers.

2.3 BOUNDARY-LAYER RAKE

The rake (Fig. 5) was composed of five probes ranging in height (distance from probe centerline to the model surface) from 0.013 to 0.40 in. Each probe had an ID of 0.010 in. and an OD of 0.014 in. at the tip. Although the rake remained at the wing trailing edge (x = 33.3 in.) throughout the test, the probes were capable of being automatically driven over a distance of 12 in. from the trailing edge along the suction area centerline. A magnet was located in the probe head to assure continuous contact with the curved model surface.

2.4 SUCTION SYSTEM

Suction (operating range from 0.04 to 0.10 psia) was provided by a 12-in. vacuum line, which was connected separately by 2-in. ID rubber pipe to each of the seven metering boxes (Figs. 2c and 6). Flow regulation to each suction chamber was maintained by a throttling valve on each metering box. Interchangeable nozzles facilitated measurement of different levels of mass flow from each of the seven model suction chambers.

2.5 INSTRUMENTATION

Model data recorded during the test were boundary-layer pitot pressures, model surface static pressures, suction chamber pressures and temperatures, metering chamber total pressures and temperatures, and metering nozzle static pressures. Pressures were measured with differential transducers, and data were processed with the VKF data handling system and computer to provide reduced data while the test was in progress.

3.0 PROCEDURE

Testing was conducted with variable suction and no suction at each of the following conditions:

Mach No.	Maximum Re/in. x 10^{-6}	Minimum Re/in. x 10^{-6}	α, deg
1.99	0.33	0.11	0.15
	0.33	0.11	0.45
	0.43	0.11	0.75
2.25	0.20	--	0.15
	0.097	--	0.45
	0.094	--	0.75

Boundary-layer profiles were measured for the above-listed Reynolds number ranges and angles of attack. The condition of no suction was obtained by closing the metering chamber valves and leaving the slots unsealed. The effect of varying the suction quantities through the seven chambers was observed by noting the changes in the boundary-layer profile at the rake station (x = 33.3 in.).

The following chart shows the typical suction coefficient distribution for the cases of optimum suction (lowest total drag) at three angles of attack for Mach number 2.

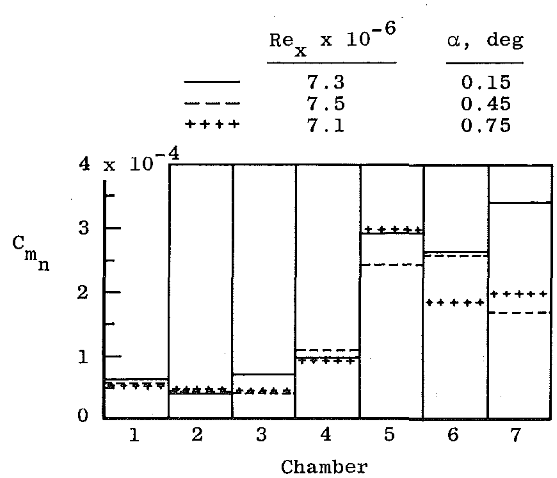

4.0 DATA ANALYSIS

Reduction of the boundary-layer data consisted of determining the momentum thickness from a graphical integration of the momentum parameter. The momentum parameter was normalized with respect to the local free-stream conditions ($\rho_r U_r$), which were determined from the measured local static pressure on the model surface and the tunnel stagnation conditions.

For a surface with zero pressure gradient ($U_r = U_\infty$), the wake drag coefficient, which is the skin friction coefficient per unit span, is determined from

$$C_{D_W} = \frac{2\,\theta_\infty}{x} = \frac{2\,\theta_r}{x} \tag{1}$$

where x is the distance (measured in flow direction) of the boundary-layer rake from the model leading edge. If the conditions outside the boundary layer at the rake location differ from free stream ($U_r \neq U_\infty$) and the momentum equation of the wake is solved, then the wake drag coefficient (composed of skin friction and form drag) can be expressed by Eq. (1) and a correction factor that depends on the local and free-stream flow conditions as shown in Ref. 2. At all test conditions this correction factor was less than one percent, and consequently all data in this report were reduced with Eq. (1).

The suction coefficient per unit span is defined by

$$C_{m_t} = \sum_{n=1}^{x} C_{m_n} = \sum_{n=1}^{x} \frac{m_n}{\rho_\infty\, U_\infty\, A_n} \tag{2}$$

Consideration of the reduction in skin friction drag by using suction must necessarily include an evaluation of the penalties in drag caused by suction. The total drag coefficient then consists of a summation of the wake drag and suction drag coefficients ($C_{D_W} + C_{D_S}$).

The suction drag coefficient is determined by the power required to accelerate the air removed from the boundary layer to free-stream conditions and is based on the assumption that the flow is isentropic and the efficiency of the suction compressor is equal to the propulsive efficiency of the propulsion system. The suction drag coefficient can be expressed as shown in Ref. 2 by

$$C_{D_S} = \sum_{n=1}^{x} \left(C_{D_S}\right)_n = \sum_{n=1}^{x} C_{m_n} \left(1 + \frac{M_n^2\, T_n}{M_\infty^2\, T_\infty}\right) \tag{3}$$

where C_{D_S} is the suction drag coefficient.

An alternate procedure for evaluating the suction drag consists of assuming that all the momentum removed from the boundary layer is lost, and the suction drag coefficient thus determined is

$$C_{D_S} = \sum_{n=1}^{x} \frac{\text{suction drag}}{q_\infty A_n} = \sum_{n=1}^{x} \frac{m_n U_\infty}{\frac{1}{2} \rho_\infty U_\infty^2 A_n} = 2 \sum_{n=1}^{x} C_{m_n} \qquad (4)$$

These two methods determine the limits on suction drag. Shown below are the suction drag coefficients applied to typical data and the total drag coefficients for the two methods of evaluating suction drag:

M_∞	α, deg	$Re_x \times 10^{-6}$	$C_{D_W} \times 10^4$	$C_{D_S} \times 10^3$	$C_{D_T} = (C_{D_W} + C_{D_S}) \times 10^3$
1.99	0.45	7.5	4.608	Eq. (3) 1.072	1.533
1.99	0.45	7.5	4.608	Eq. (4) 1.826	2.287

All suction drag coefficients used in this report were determined from the relationships expressed by Eq. 3.

5.0 RESULTS AND DISCUSSION

It was mentioned previously that the wing was mounted vertically to a horizontal support plate that was contoured to coincide with the flow field streamlines. The support plate contour would minimize the adverse effects resulting from the junction of the wing and support plate. Presented in Fig. 7 are the model surface pressure distributions obtained at M_∞ = 1.99 and 2.25, α = 0.45 deg, and three spanwise stations for the conditions of suction and no suction. These data show that the pressure distributions along the three spanwise locations were essentially equal, and consequently the support plate contouring was successful in establishing two-dimensional flow over the wing test section. The theoretical pressure distribution shown in Fig. 7 was determined by Goldsmith (Ref. 3) using a modified version of the Theodorsen method (Ref. 4) by applying a compressibility factor based on (M_∞ cos 72.5 = 0.6). At M_∞ = 2 and α = 0.45 deg, good agreement exists between theory and the experimental results. There was no noticeable difference in surface pressure for the conditions of suction and no suction except over the last 10 percent of the wing chord. For the case of no suction at M_∞ = 2.25, the pressure at span station 3 and x/c = 1.0 was approximately 16 percent lower than the pressure for the suction case. This suggests a possible separated flow region caused by the high pressure gradient that existed aft of the 70 percent chord or adverse effects from the strong spanwise flow. Also shown are the theoretical pressure ratios for which the local Mach number component (M_{rN}) outside the boundary layer and perpendicular to the wing leading edge would become sonic, and consequently shocks would form and suction would be ineffective. Note that at $M_\infty = 2.25$ the critical pressure ratio was almost obtained.

Presented in Fig. 8 are typical laminar boundary-layer velocity and momentum profiles for Mach numbers 1.99 and 2.25, $\alpha = 0.45$ deg, at rake station 33.3 in. for optimum suction conditions (lowest total drag). As seen from the figures, optimum suction was adequate to establish full chord laminar flow at both test Mach numbers.

The variations in wake drag, suction drag, and total drag coefficients for various total suction coefficients are presented in Fig. 9 for Mach number 1.99 and $\alpha = 0.15$, 0.45, and 0.75 deg. With increased suction the wake drag will decrease, but the suction drag increases, and therefore a minimum value will exist for the total drag coefficient ($C_{D_T} = C_{D_W} + C_{D_S}$). This point represents the minimum total drag coefficient and defines the optimum suction coefficient.

The minimum total drag coefficients and optimum suctions coefficients for $M_\infty = 1.99$ and 2.25, $\alpha = 0.15$, 0.45, and 0.75 deg are presented in Fig. 10. Full chord laminar flow was maintained for $M_\infty = 1.99$ at all three angles of attack up to a length Reynolds number of approximately 9×10^6. Above a Reynolds number of 10×10^6, the flow became turbulent at the rake which resulted in a sharp rise in total drag that is associated with transition from laminar to turbulent flow. As seen from the figure, there was only a small difference in the optimum suction coefficients and minimum total drag coefficients for the changes in angle of attack. For comparative purposes a few data points are presented for $M_\infty = 2.25$ and show that higher suction quantities were required to establish laminar flow with correspondingly slightly higher total drag values than existed at $M_\infty = 2$.

6.0 CONCLUDING REMARKS

Tests were conducted at Mach numbers 1.99 and 2.25 to determine the effectiveness of boundary-layer suction for laminar flow control on a 72.5-deg swept wing having a subsonic leading edge. On the basis of these tests the following conclusions are made:

1. Measurements of the chordwise pressure distribution at three spanwise stations showed that the flow was two-dimensional.

2. Full chord laminar flow was established and maintained at $M_\infty = 1.99$, $\alpha = 0.15$, 0.45, and 0.75 deg at length Reynolds numbers up to approximately 9 million.

REFERENCES

1. Coats, Jack D. "Flow Characteristics of a 40-Inch Wind Tunnel at Mach Numbers 1.5 to 6." AEDC-TDR-62-130, June 1962.

2. Groth, E. E. "Boundary Layer Suction Experiments at Supersonic Speeds." Boundary Layer and Flow Control, edited by Lachmann, G. V., Vol. 2, Pergamon Press, New York, Oxford, London, Paris, 1961.

3. Goldsmith, John. "IBM Computer Program for Calculating Velocity and Pressure Distributions On or Near a Two-Dimensional Airfoil." NOR-61-214, September 1961.

4. Theodorsen, Theodore. "Theory of Wing Sections of Arbitrary Shape." NACA Report 411, 1932.

5. van Driest, E. R. "Turbulent Boundary Layer in Compressible Fluids." Journal of the Aeronautical Sciences, Vol. 18, No. 3, March 1951, pp. 145-160, 216.

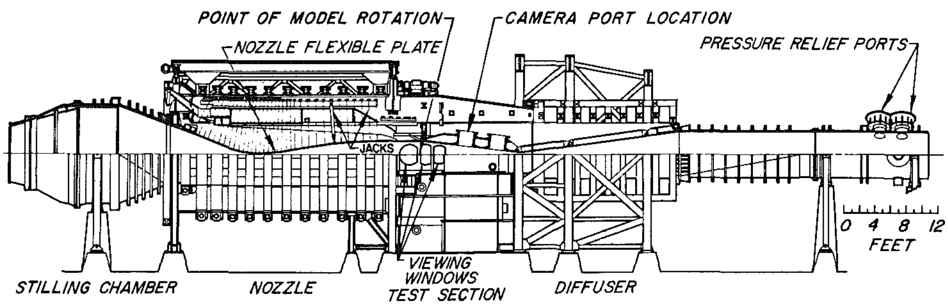

Assembly

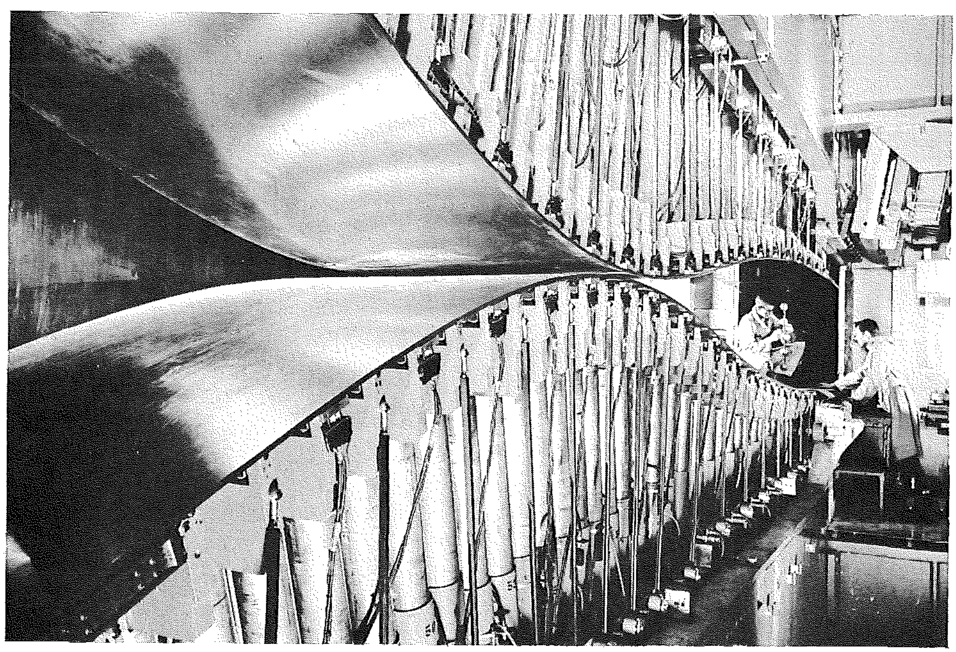

Nozzle and Test Section

Fig. 1 The 40-Inch Supersonic Tunnel (A)

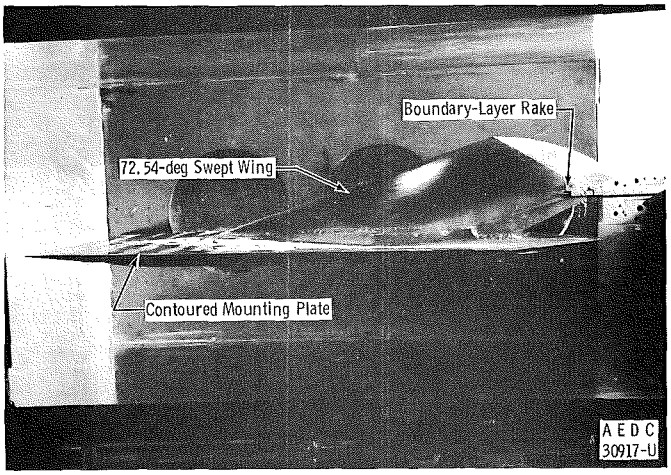

a. Model Installation, Side View

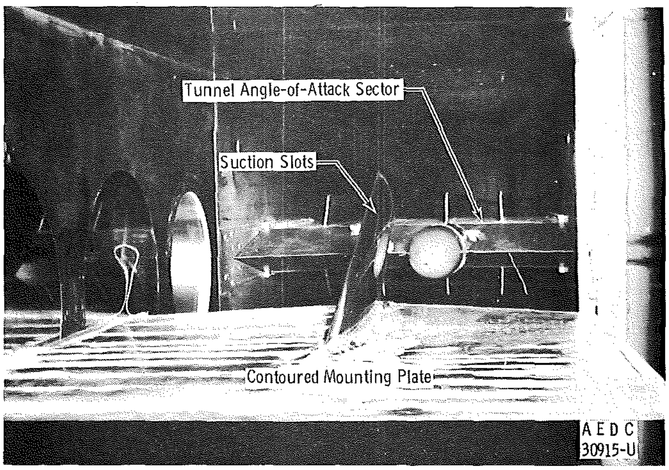

b. Model Installation, Downstream View

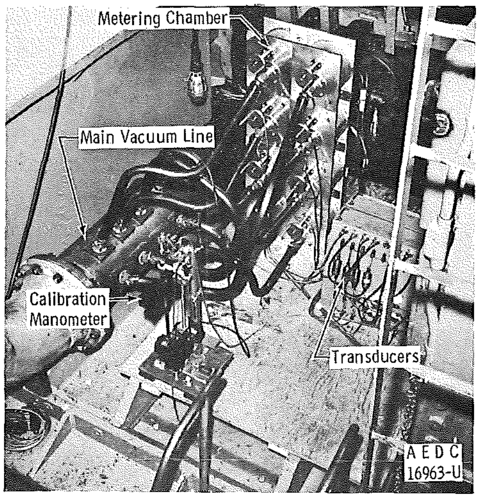

c. Suction Equipment

Fig. 2 Model Installation and Suction Equipment

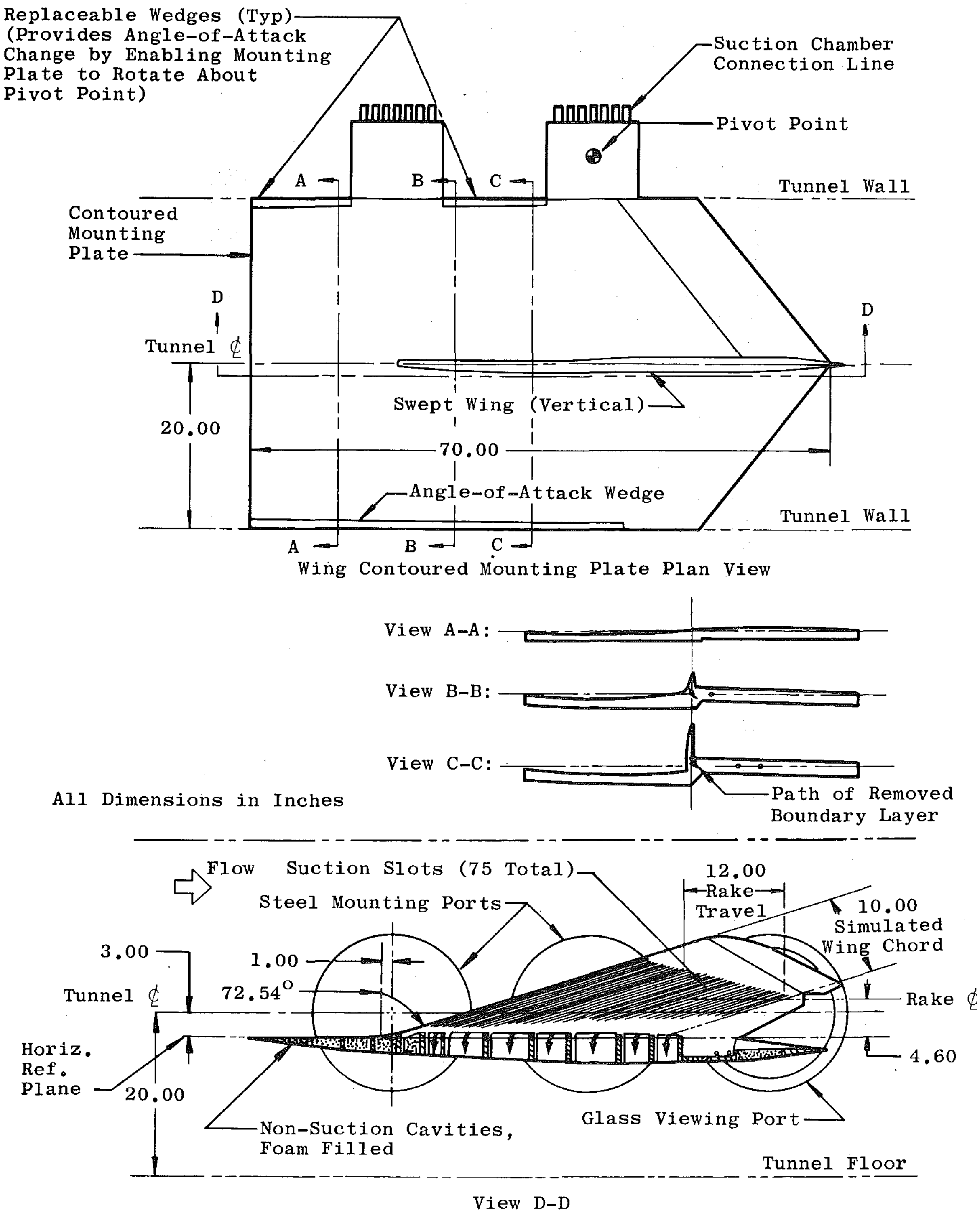

Fig. 3 Model Geometry

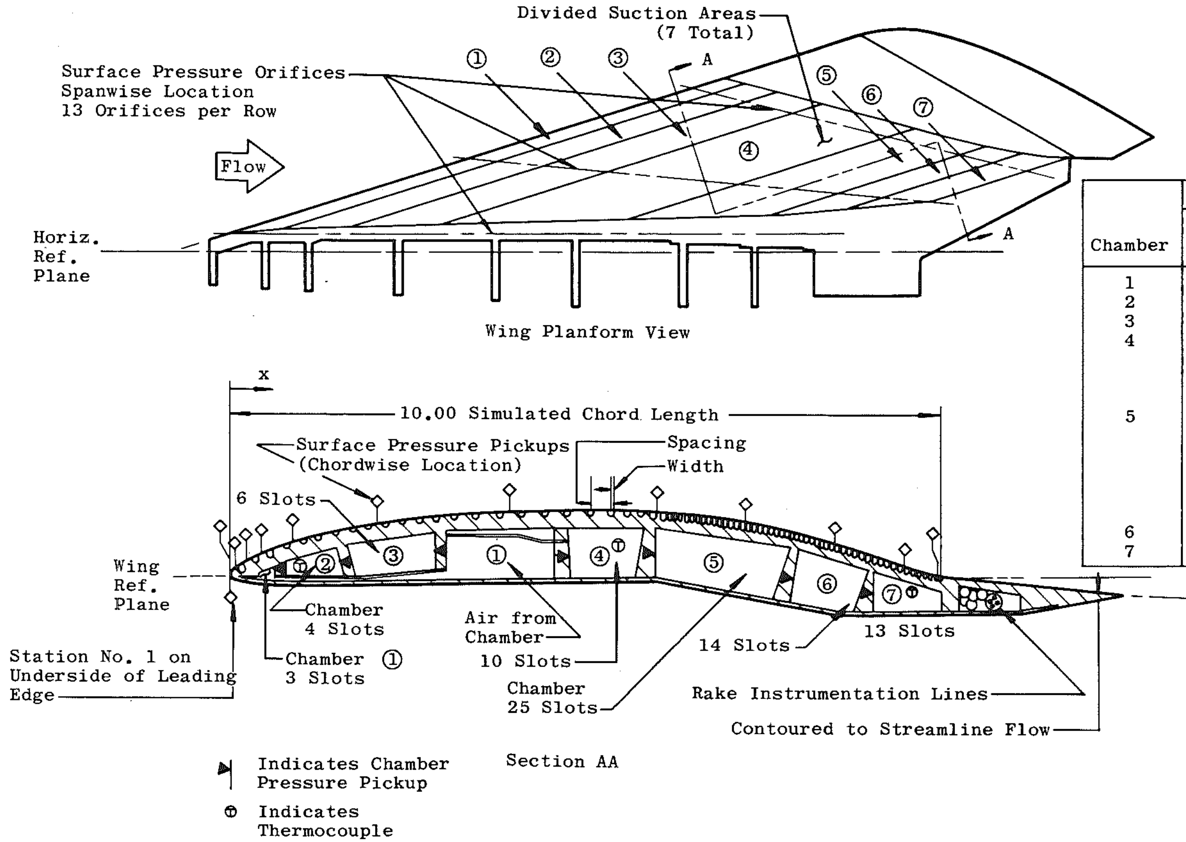

Chamber	Slot No.	Slot Spacing, in.	Slot Width, in.	Orifice No.	Orifice x/c
1	1-3	0.24	0.003	1	0.002
2	4-7	0.24		2	0.002
3	8-13	0.24		3	0.008
4	14-19	0.32		4	0.025
	20	0.28		5	0.046
	21	0.24		6	0.090
	22	0.20		7	0.210
5	23	0.15		8	0.395
	24	0.14		9	0.602
	25	0.11		10	0.728
	26,27	0.08	0.003	11	0.853
	28-41		0.004	12	0.952
	42-50		0.003	13	0.998
6	51-64				
7	65-75	0.08	0.003		

Fig. 4 Sketch of 72.5-deg Swept Wing

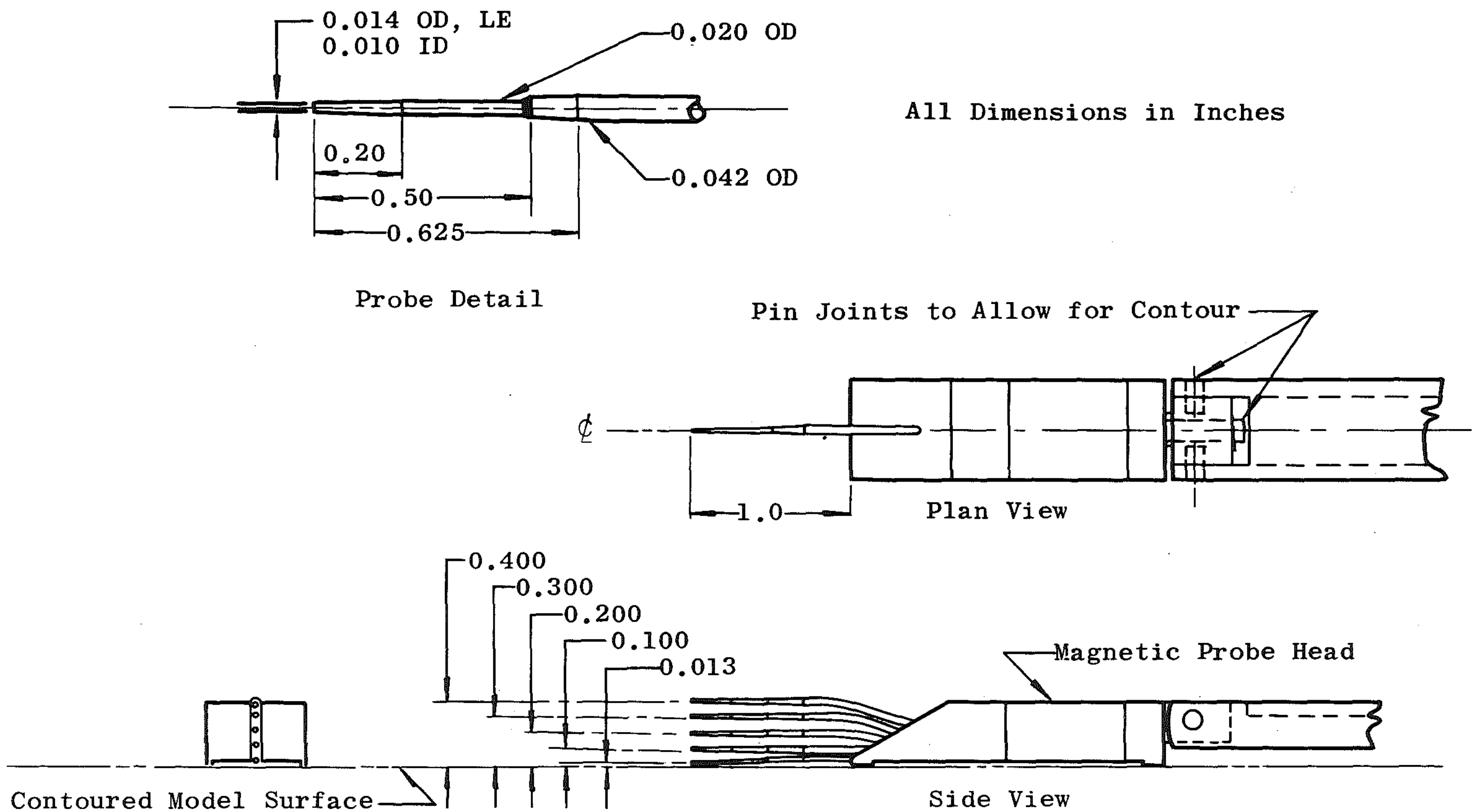

Fig. 5 Sketch of Boundary-Layer Rake

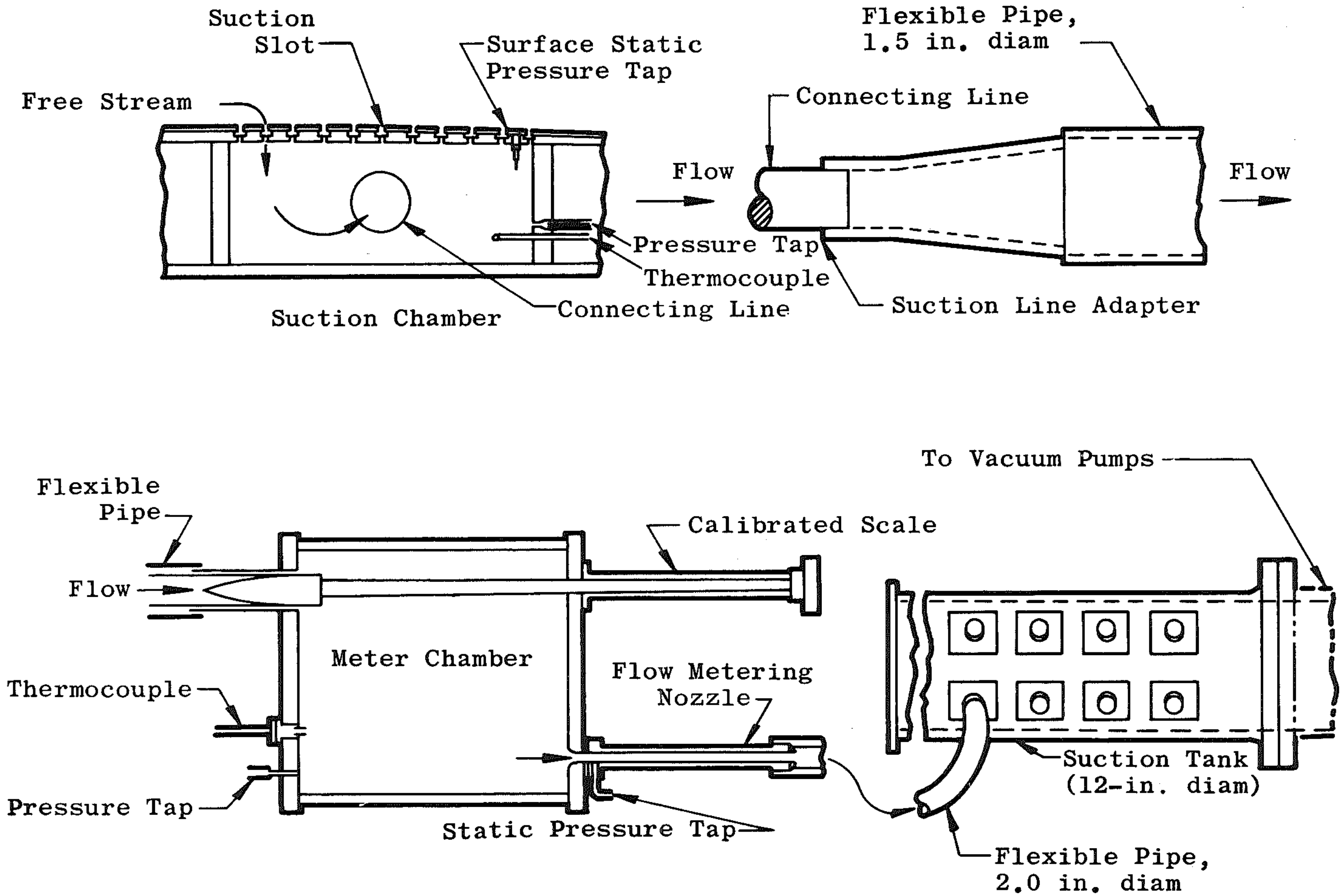

Fig. 6 Schematic Drawing of Suction System

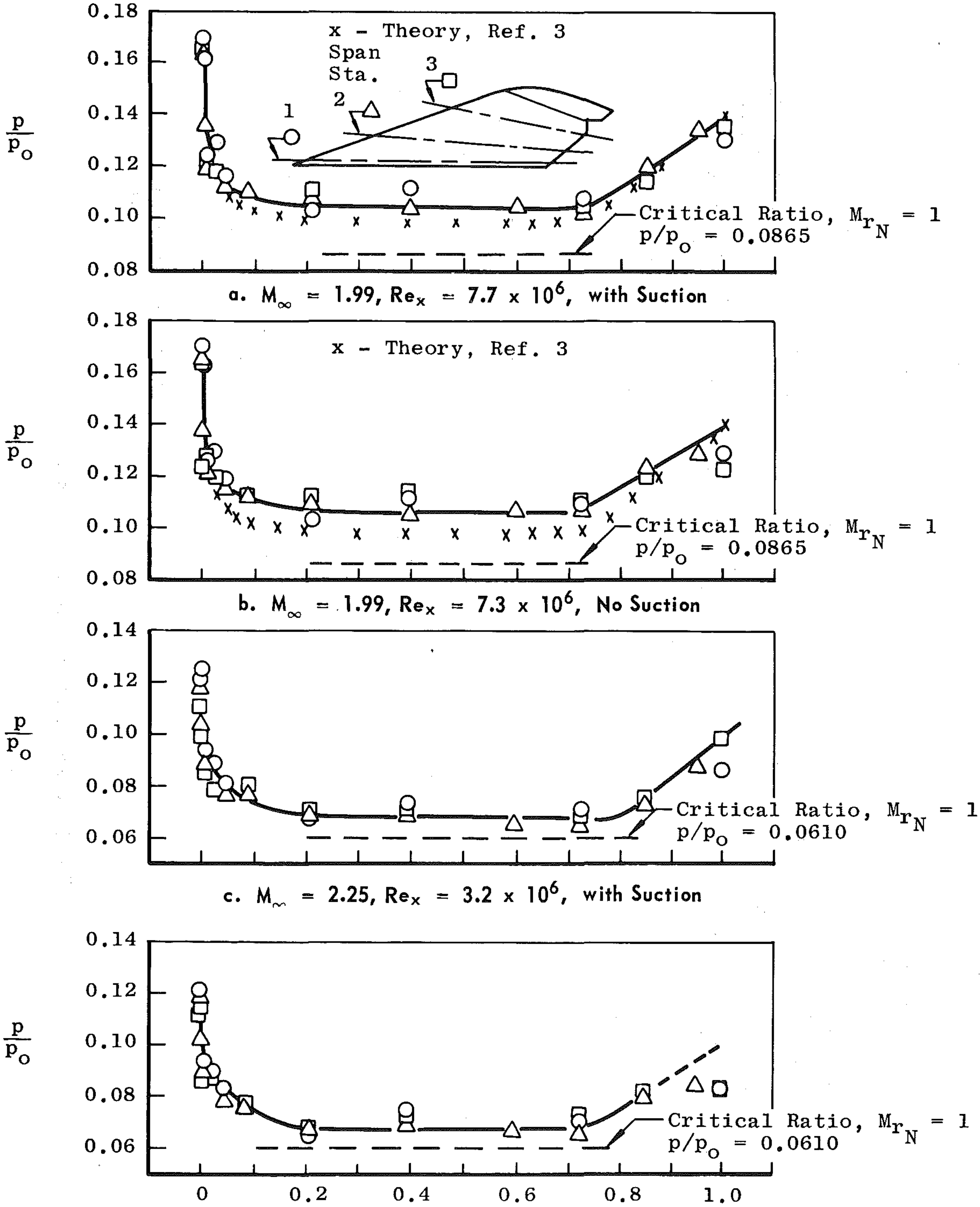

a. $M_\infty = 1.99$, $Re_x = 7.7 \times 10^6$, with Suction

b. $M_\infty = 1.99$, $Re_x = 7.3 \times 10^6$, No Suction

c. $M_\infty = 2.25$, $Re_x = 3.2 \times 10^6$, with Suction

d. $M_\infty = 2.25$, $Re_x = 3.3 \times 10^6$, No Suction

Fig. 7 Model Surface Pressure Distribution with and without Suction, $M_\infty = 1.99$ and 2.25, $\alpha = 0.45$ deg

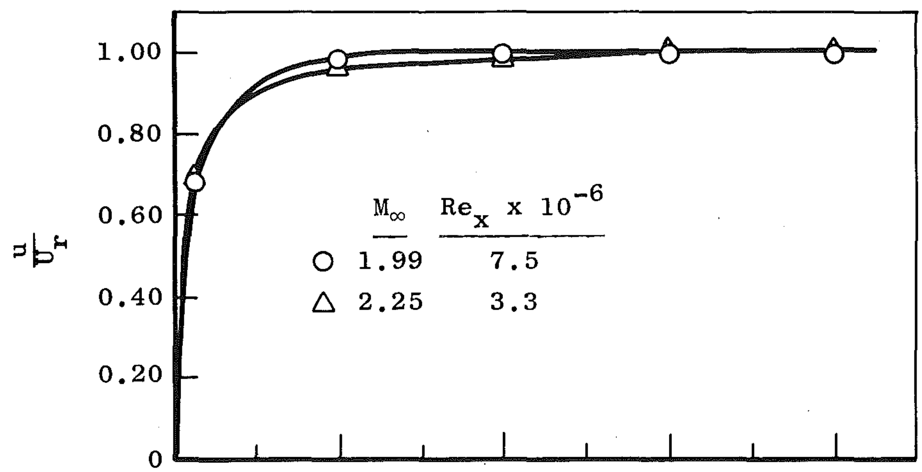

a. Velocity Profiles

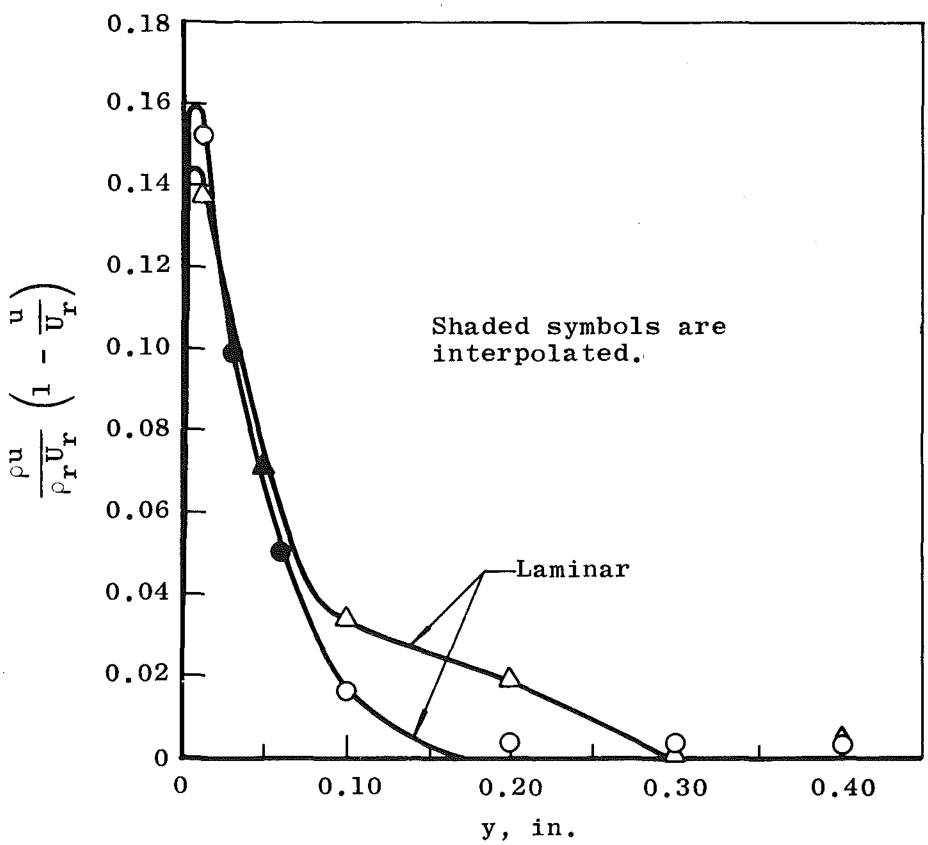

b. Momentum Profiles

Fig. 8 Boundary-Layer Profiles with Optimum Suction at M_∞ = 1.99 and 2.25, α = 0.45 deg, Rake at Station 33.3 in.

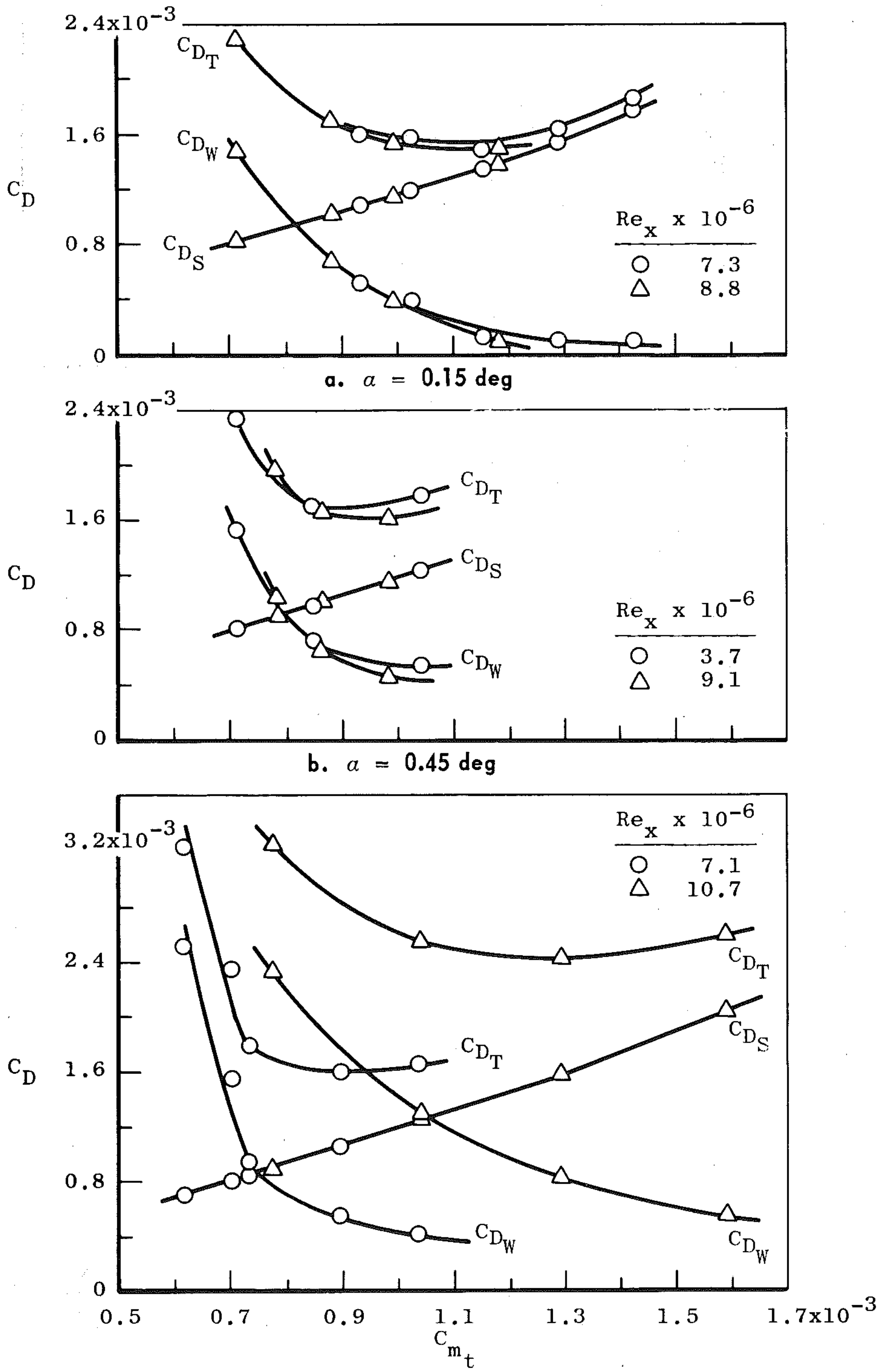

a. α = 0.15 deg

b. α = 0.45 deg

c. α = 0.75 deg

Fig. 9 Variation of Drag Coefficients with Suction Coefficients, Rake at 33.3 in., M_∞ = 1.99

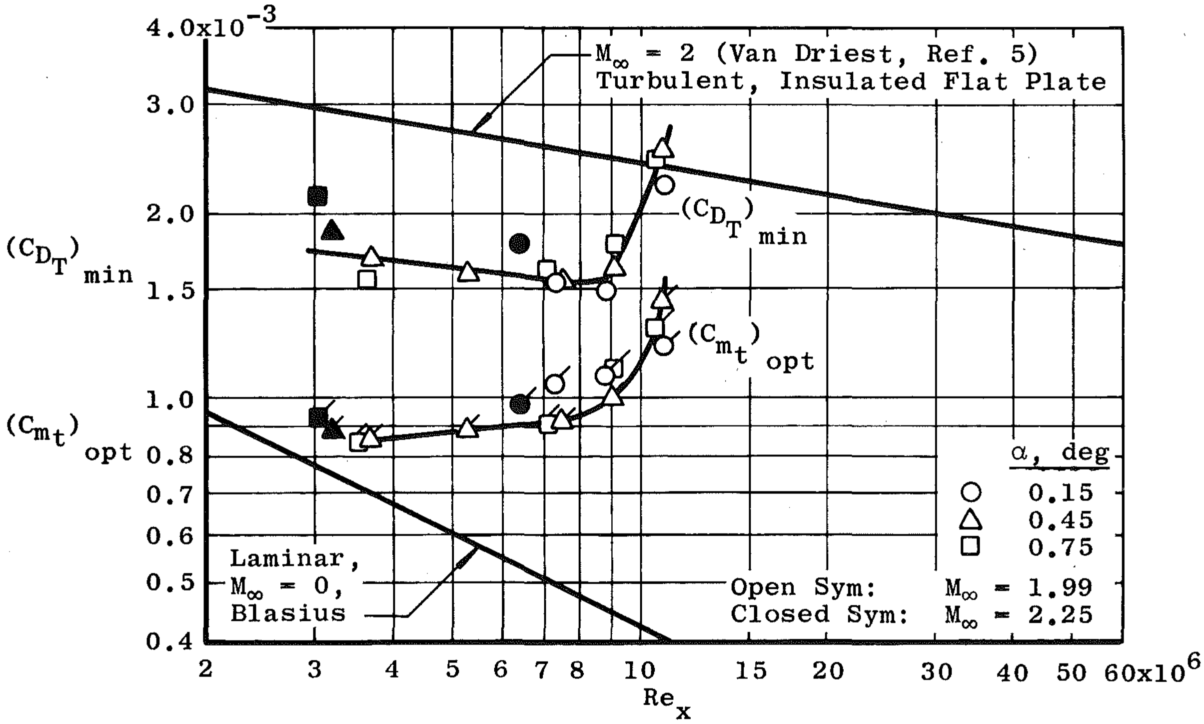

Fig. 10 Variation of Minimum Total Drag Coefficients and Optimum Suction Coefficients with Reynolds Number, Rake at Station 33.3 in.